

The effects of Ba²⁺ content on depolarization temperature and pyroelectric properties of lead-free 0.94Na_{0.5}Bi_{0.5}TiO₃–0.06Ba_{1+x}TiO₃ ceramics

A. M. Balakt¹ · C. P. Shaw¹ · Q. Zhang¹

Received: 4 May 2016 / Accepted: 25 July 2016 / Published online: 11 August 2016
© The Author(s) 2016. This article is published with open access at Springerlink.com

Abstract Lead-free 0.94Na_{0.5}Bi_{0.5}TiO₃–0.06Ba_{1+x}TiO₃ (NBT–0.06B_{1+x}T) ceramics (0.0 ≤ x ≤ 0.03) were synthesized by a conventional solid-state reaction process. X-ray diffraction shows that the compositions are at the morphotropic phase boundary where rhombohedral and tetragonal phase coexist. Grain size slightly changes with the increase of Ba²⁺ content and reaches the minimum at x = 0.02. The depolarization temperature (T_d) decreases with the extra Ba²⁺ content but the lowest T_d was obtained at x = 0.01–0.02. The pyroelectric coefficient (p) was measured as a function of Ba²⁺ content, and increased from 2.90×10^{-4} to 3.54×10^{-4} C m⁻² °C⁻¹, and from 55.3×10^{-4} to 740.7×10^{-4} C m⁻² °C⁻¹ for x = 0.00 and 0.02 at RT, and depolarization temperature (T_d) respectively. The pyroelectric coefficient (p) shows a large increase with rising the temperature and reaches the maximum value at the depolarization temperature (T_d). The figures of merits of F_i , F_v and F_D have all been improved with the addition of extra barium. These improved pyroelectric properties indicate that NBT–0.06B_{1+x}T is a promising material for pyroelectric applications or a wide range of temperature.

1 Introduction

At present the most widely used ferroelectric materials are lead-based ceramics such as PZT and PZT-based multi-component ceramics due to their superior piezoelectric and electrical properties, but there are two serious

environmental problems arising from the fabrication of lead-containing materials: atmospheric pollution caused by PbO vapour during ceramic fabrication, and the difficulty in removing lead during component recycling. Lead-containing electronic products have been banned in WEEE (waste electrical and electronic equipment) and ROHS (restriction of use of certain hazardous substances) legislation [1]. Therefore there is a need to develop lead-free materials with properties comparable to lead-based ceramics. Among the lead-free materials, sodium bismuth titanate (Na_{0.5}Bi_{0.5}TiO₃, (NBT)) and NBT-based materials are considered to be an important material for the fabrication of lead-free material [2–5] due to their excellent ferroelectric and dielectric properties [5]. Large efforts of investigation on NBT-based materials for their piezoelectric applications have been made while there have been limited reports on their pyroelectric properties.

Pyroelectric ceramic materials are becoming increasingly on high demand in variety of industrial applications such as sensors, infrared detectors, thermal cameras, gas detectors, microelectronic devices, as well as actuators, transducers, medical devices, airplanes and spacecraft [6]. These materials could have a large pyroelectric coefficient (polarization change vs temperature change) at a phase transition temperature. NBT exhibits two structural phase transitions: the first one (T_d) from a ferroelectric rhombohedral to a tetragonal phase (~260–350 °C) and the second one (T_c) from a tetragonal phase to a paraelectric cubic phase (520–540 °C). These phase transition temperatures are well above room temperature. Hence it is necessary to bring the phase transition temperature down to near room temperature (RT) for many applications, and that can be achieved by using various dopants [7]. In NBT-based systems, there is a weakly polar intermediate phase [8],

✉ Q. Zhang
q.zhang@cranfield.ac.uk

¹ School of Aerospace, Transport and Manufacturing, Cranfield University, Cranfield, Bedfordshire MK43 0AL, UK

which occurs between the depolarization temperature T_d and the temperature of maximum permittivity (T_m) [9–12].

$(1-x)(\text{Na}_{0.5}\text{Bi}_{0.5})\text{TiO}_3-x\text{BaTiO}_3$ has a morphotropic phase boundary at $x = 0.06\text{--}0.07$ [13] and its depolarization temperature (T_d) is ~ 123 °C and well below its phase transition temperature (T_m) which is around 300 °C. Jo et al. [14] reported that T_d could be the phase transition temperature from ferroelectric to relaxor or from rhombohedral ferroelectric to tetragonal ferroelectric [12]. This phase transition at T_d may induce a large pyroelectric effect. Guo et al. [15] studied the pyroelectric properties of $(1-x)\text{NBT}-x\text{Ba}(\text{ZrTi})\text{O}_3$ ($0 \leq x \leq 0.12$) ceramics and found that the pyroelectric coefficient was enhanced from $0.057 \mu\text{C cm}^{-2} \text{ }^\circ\text{C}^{-1}$ at RT to $2.21 \mu\text{C cm}^{-2} \text{ }^\circ\text{C}^{-1}$ at T_d (87 °C). In this work, we aim to bring down the T_d by varying the Ba^{2+} content in $0.94(\text{Na}_{0.5}\text{Bi}_{0.5})\text{TiO}_3-0.06\text{Ba}_{1+x}\text{TiO}_3$ ($\text{NBT}-0.06\text{B}_{1+x}\text{T}$) ceramics and to investigate the effect of Ba^{2+} content on the depolarization temperature, and the subsequent dielectric and pyroelectric properties at T_d .

1.1 Experimental

A solid state synthesis route was used to prepare $\text{NBT}-0.06\text{B}_{1+x}\text{T}$ composition. The raw materials used in this project were powders, bismuth oxide (Bi_2O_3 , 99.999 %), sodium carbonate (Na_2CO_3 , 99.5 %), barium carbonate (BaCO_3 , 99.98 %), and Titanium dioxide (TiO_2 , >99.8 %). All chemicals were purchased from Sigma-Aldrich, UK.

The amounts of powders were calculated according to the chemical formula of $0.94\text{Na}_{0.5}\text{Bi}_{0.5}\text{TiO}_3-0.06\text{Ba}_{1+x}\text{TiO}_3$ with $x = 0.00, 0.01, 0.02,$ and 0.03 . The raw materials were ball-milled in acetone for 24 h. in order to mix and mill the powders. The resultant slurries were dried at 50 °C for 8 h. The dried powder cakes were ground in a mortar for 10 min. and sieved through a 250 μm mesh in order to aid the calcination. The powders were calcined at 850 °C for 180 min at a heating ramp rate of 1 °C per min and cooling rate 5 °C per min in a furnace. After calcination, powders were re-milled for 24 h. in acetone, and 2 % of poly vinyl alcohol (PVA) was added as an organic binder to the dried powders to enhance the mechanical strength of the particles. After that the powders were dried in oven at 80 °C until fully dried. The dried powders were ground and sieved and subsequently pressed into green pellets with a diameter of 10 mm under an uniaxial compaction with load ~ 78 MPa for 5 min at RT . The pellets were sintered at temperatures up to 1150 °C in closed crucibles in order to minimize the loss of volatile Na^+ and Bi^{3+} . The pellets were manually wet polished on both sides using silicon carbide paper to improve uniformity

and dried at 100 °C overnight to remove the moisture. Silver conductive paint (RS limited) was used to electrode the pellets, and electrical poling at 5.5–6 kV/mm for 10 min at RT in silicone oil was carried out using a Keithley (6517 Electrometer/high resistance) dc power supply.

SEM (FEI XL30 SFEG) was used to look at the surface morphology of the sintered samples and X-Ray Diffraction (XRD) (Siemens Ltd Model: D500) was used to investigate microstructure. As part of the electrical characterisation of the materials, dielectric measurements were made using an impedance analyser (Wayne kerr Electronics Ltd. Model 3245 and Hewlett Packard HP4092A). Dielectric data was collected over a temperature range from RT to 150 °C using a temperature controlled hotplate in the frequency range of 0.1–10 kHz. Pyroelectric measurements were made using the Byer-Roundy [16] method at the temperature between 20 and 90 °C (equipment up limitation) under vacuum and the pyroelectric current was collected by a Keithley electrometer (Model 6217). Dielectric and pyroelectric data was then used to study the phase changes such as depolarization temperatures (T_d), and to determine figure of merit values F_i , F_v and F_D .

Sample compositions are listed in Table 1.

2 Results and discussion

2.1 Effects of extra barium on microstructure

Figure 1 shows the XRD patterns of $0.94\text{NBT}-0.06\text{B}_{1+x}\text{T}$ ($\text{NBT}-0.06\text{B}_{1+x}\text{T}$) ceramic powders calcined at 850 °C for 3 h. Figure 1a showed that all ceramic samples have a pure perovskite structure (ABO_3) and no second phase was observed. The absence of other phase indicates that $\text{NBT}-0.06\text{B}_{1+x}\text{T}$ lattices have either absorbed the extra amount of Barium (Ba^{2+}), and formed the $\text{NBT}-0.06\text{B}_{1+x}\text{T}$ ceramic solid solutions [17, 18] or the amount of the second phase is too small to be tested by XRD. Figure 1 shows, in all the samples, a splitting in the peak [111] into [003] and [021] at $39.0^\circ\text{--}41.0^\circ$, indicating the existence of rhombohedral phase (Fig. 1b) and a splitting in the peak [200] into [200] and [002] at $45.0^\circ\text{--}48.0^\circ$, indicating the existence of tetragonal phase (Fig. 1c). The coexistence of both rhombohedral and tetragonal phases in $\text{NBT}-0.06\text{B}_{1+x}\text{T}$ ceramics proves that the sample structures are at morphotropic phase boundary (MPB), which was consistent with what was reported in literature [12, 14, 19]. Figure 1c shows that the splitting in peak [200] became quite pronounced for the sample at $x = 0.02$ as shown in Fig. 1b. It seems that the composition of $\text{NBT}-0.06\text{B}_{1+x}\text{Ti}$ with $x = 0\text{--}0.03$ is still within MPB.

Table 1 The NBT–0.06B_{1+x}T₁ composition (sample) depending on the extra concentrations of Ba²⁺ from A, x = 0.00 to D, x = 0.03; samples density (gm cm⁻³), comparing with the theoretical density (%) which is (ρ = 6 gm cm⁻³), and the relative permittivity (ε_r),

| Composition (sample name) | Lattice parameters (Å) | | | Density (ρ) gm cm ⁻³ | Compare with theoretical density% | Depolarization temperature (T _d) (°C) | Relative permittivity (ε _r) at RT | Dielectric loss (tanδ) at RT |
|---|------------------------|--------|-------|---------------------------------|-----------------------------------|---|---|------------------------------|
| | a = b | c | | | | | | |
| NBT–0.06BT (A, x = 0.0) | 5.488 | 13.505 | 5.697 | 94.95 | 125 | 1178 | 0.042 | |
| NBT–0.06B _{1+0.01} T (B, x = 0.01) | 5.487 | 13.437 | 5.661 | 94.35 | 85 | 1468 | 0.046 | |
| NBT–0.06B _{1+0.02} T (C, x = 0.02) | 5.494 | 13.505 | 5.718 | 95.55 | 85 | 1472 | 0.045 | |
| NBT–0.06B _{1+0.03} T (D, x = 0.03) | 5.493 | 13.505 | 5.678 | 94.63 | 115 | 1266 | 0.040 | |

dielectric loss (tanδ) both at 1 kHz and RT the depolarization temperature (T_d) values 0.0 ≤ x ≤ 0.03 in present work and from the literatures

The measurement of the lattice parameters (a, b and c) reveals that the extra Ba content has slightly changed a, b and c from a = b = 5.488 Å, c = 13.505 Å to a = b = 5.493 Å, c = 13.505 Å for Samples A to D respectively (Table 1). Sample C presents the biggest lattice parameters (a = b = 5.494 Å, c = 13.505 Å).

Comparing the ionic radii of the A-site cations of Na⁺ (1.39 Å), Bi³⁺ (1.31 Å) and Ba²⁺ (1.61 Å) (coordination No. 12) according to Hume-Rothery rules, Ba²⁺ in NBT–0.06B_{1+x}Ti could replace Na⁺ but seems to be difficult to replace Bi³⁺ because the radius difference between Bi³⁺ and Ba²⁺ is more than 15 % [19]. Yoon et al. [19] reported that the c/a ratio increased with adding more extra Ba content and reached the maximum at x = 0.02. Thus the increase in Ba²⁺ content would lead to the improvement of the tetragonality of BT in NBT–0.06B_{1+x}T by compensating for the loss in Ba during the sintering stage. However, any extra Ba²⁺ content more than x = 0.02 would not go to increase the c/a ratio because the c/a ratio was saturated at 0.02, and therefore consequently the extra Ba would precipitate into a secondary phase [19], but in this study the second phase was not identified up to x = 0.03, probably due to the amount of the secondary phase being too small to be tested by XRD.

Figure 2 shows the surface morphology of the NBT–0.06B_{1+x}T ceramics by SEM. The average grain size was reduced from 1.7 μm at x = 0.00 to 1.61, 1.31, 1.52 at x = 0.01, 0.02 and 0.03, respectively. Increasing Ba²⁺ led to a sharp reduction in the grain size and reached the lowest value at x = 0.02. In general, Ba²⁺ behaves as an inhibitor of the grain growth in NBT system. In lead-based ceramics, such as PZT and PLZT (La-containing PZT), similar effect was also observed when lead was substituted with barium [17, 19, 20]. All the samples showed a density 94.63 ± 0.333 g/cm³ as shown in Table 1. Density measurements revealed that Sample A, B and D at x = 0.0,

0.01 and 0.03 have a similar density value; however, Sample C, at x = 0.02 has a higher density.

2.2 Effects of extra barium on dielectric properties

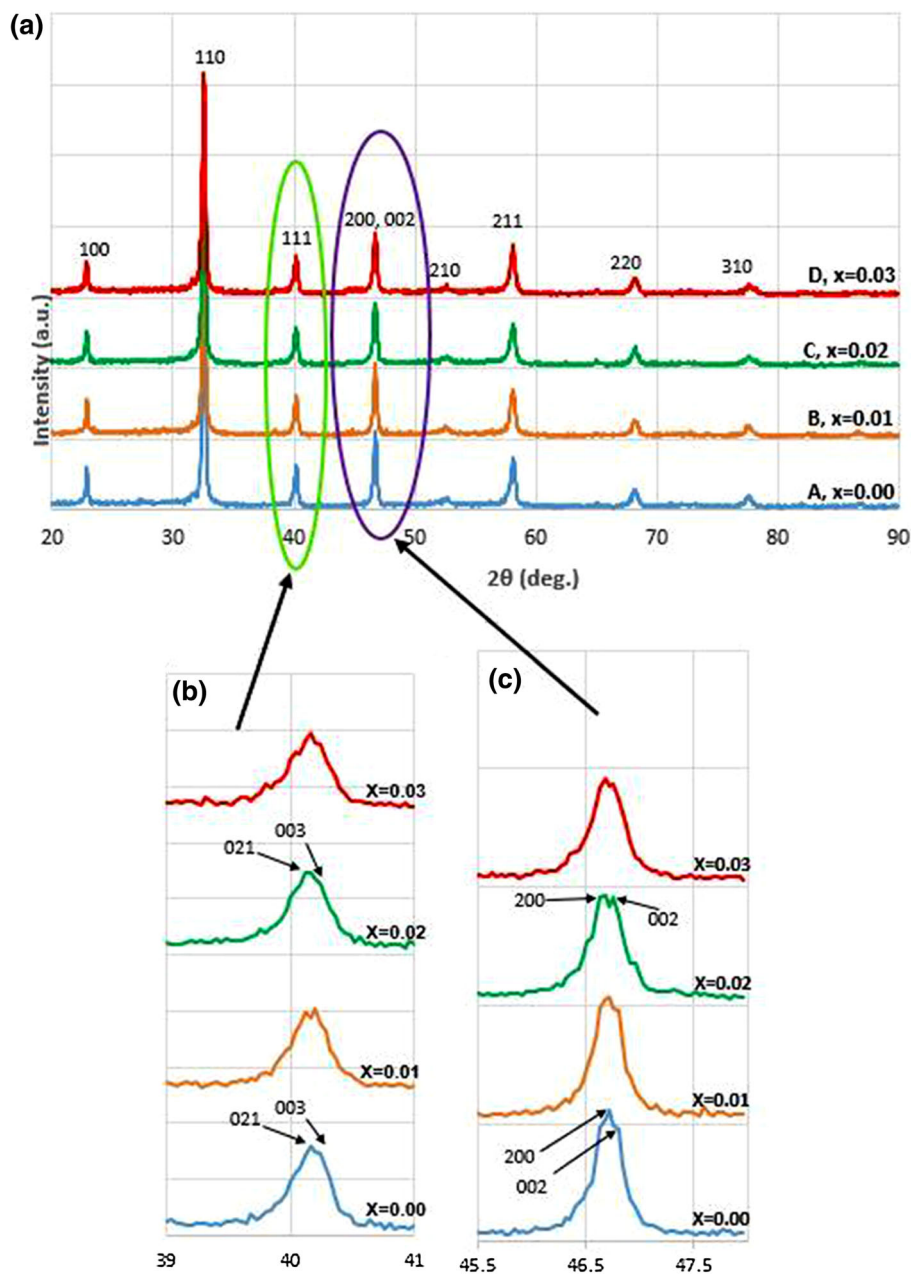
Figure 3 shows the temperature dependence of the dielectric properties of poled NBT–0.06B_{1+x}T from RT up to 150 °C at different frequencies (1, 10 and 100 kHz). The relative dielectric permittivity (ε_r) and the dielectric loss tangent (tanδ) show a strong dependence upon Ba content and temperature. The ε_r increased with temperature for all samples; however, the ε_r showed increasing at x = 0.01, and 0.02 at room temperature and this can be related to extra Ba²⁺. The extra Ba at x = 0.01 compensated the deficiency in Ba in BT side and rectified the tetragonality in NBT. The excess Ba up to 0.02 can then replace cations in the A-site of the NBT–0.06B_{1+x}T perovskite structure, so Ba²⁺ will replace Na⁺ according to the radius matching rules and the donor behaviour of Ba will make the domain wall motion easier resulting in the increase of the dielectric properties of NBT–0.06B_{1+0.02}T [12].

The ε_r values at x = 0.01 and 0.02 were close to 1500 for both compositions whereas the ε_r values at x = 0.0 and 0.03 at RT were near 1225. However, at T_d, and 150 °C, the ε_r for the samples at x = 0.01 and 0.02 increased to around 2000 and 2150 (T_d), and above for both compositions 2500 (150 °C) respectively. However, the ε_r values for the samples at x = 0.00 and 0.03 were relatively low, which are around 2250.

2.3 Effects of extra barium on depolarization temperature

Depolarization temperature (T_d) is a parameter that has not clearly been defined [10], but the European standard on piezoelectric properties has defined it as the reduction of

Fig. 1 XRD patterns of NBT–0.06B_{1+x}TiO₃ ceramics where, **a** $x = 0.00, 0.01, 0.02$ and 0.03 ; **b** expansion at 2θ from 39.6° to 40.6° and **c** expansion at 2θ from 45.0° to 48.0°



remnant polarization because of temperature and other influences [21]. However, there are other definitions of T_d such as the steep reduction of remnant polarization [7], or the phase transition temperature from ferroelectric (*FE*) to anti-ferroelectric (*AFE*) or to relaxor anti-ferroelectric or to relaxor [8, 22–25].

In this study, T_d was identified from the measurement of the dielectric loss ($\tan\delta$) versus temperature. Figure 3 shows that the T_d of the NBT–0.06B_{1+0.00}T was at $\sim 125^\circ\text{C}$ and decreased to $\sim 85^\circ\text{C}$ at $x = 0.01$ and 0.02 , and then rises to $\sim 115^\circ\text{C}$ at $x = 0.03$. The reduction in T_d is probably due to the formation of A-site vacancies with increasing Ba content in NBT–0.06B_{1+x}T structures. In

ferroelectric NBT–BT perovskite structure, the ferroelectric domain stability is affected by the coupling between ferroelectric (BO_6) and A-site cations, and the stability of the ferroelectric domains will be reduced when vacancies are generated between the octahedral (BO_6) ferroelectric and A-site cations. In this study, Ba^{2+} content at $x = 0.01$ – 0.02 created A-site vacancies so the stability of the ferroelectric domain reduced as a result inducing the phase change from ferroelectric (*FE*) to relaxor anti-ferroelectric (*relaxor AFE*) and fast reduction by 40°C in depolarization temperature (T_d) [14, 18, 21]. With a further increase of Ba^{2+} to $x = 0.03$, which is more than Ba^{2+} saturation content ($x = 0.02$), the T_d was decreased by only

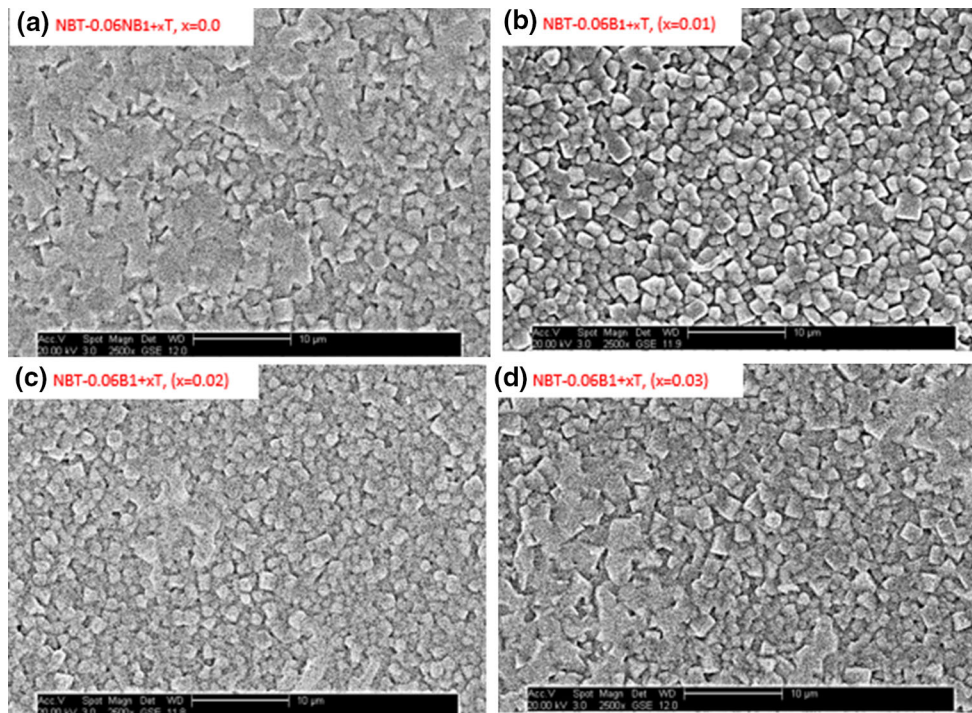


Fig. 2 The SEM surface morphology, NBT–0.06B_{1+x}T where, x = 0.00 (a); x = 0.01 (b); x = 0.02 (c); x = 0.03 (d)

about 10 °C, because there were less vacancies in A-site due to minimal (Ba²⁺/Na⁺) replacement and more ferroelectric domain wall stability [9, 14, 26]. The value of the T_d of NBT–0.06BT in this work is close to that reported in the literature (~123 °C) but the depolarization temperature of the NBT–0.06B_{1+x}T, (0.01 ≤ x ≤ 0.02) is lower than 123 °C [27]. Table 1 lists the values of relative dielectric permittivity (ϵ_r) and dielectric loss ($\tan\delta$) at RT and depolarization temperatures (T_d) at 1 kHz achieved in this work.

2.4 Effects of extra barium on the pyroelectric properties

The calculation of the figure of merits (*FOMs*) is based on the values of pyroelectric coefficient (p), relative dielectric permittivity (ϵ_r), the dielectric loss tangent ($\tan\delta$) and the specific heat (C_v). There are several numbers of *FOMs* which are more appropriate to certain pyroelectric materials applications [6, 27] and are derived from these application requirements.

Pyroelectric coefficient (p) and the *FOMs* were analysed by using the following equations: [5, 15, 28]

$$I_p = pA \frac{dT}{dt} \tag{1}$$

$$F_i = \frac{p}{C_v} \tag{2}$$

$$F_v = \frac{p}{C_v \epsilon_o \epsilon_r} \tag{3}$$

$$F_D = \frac{p}{C_v \sqrt{\epsilon_o \epsilon_r \tan\delta}} \tag{4}$$

where T is absolute temperature, t the time, I_p the pyroelectric current, F_i the high current (i) detectivity figure of merit, F_v the high voltage (V) detectivity figure of merit, F_D high detectivity figure of merit, and C_v the specific heat (2.8 JK⁻¹ cm⁻³, quoted fm [29]).

The pyroelectric current of NBT–0.06B_{1+x}T, (0.00 ≤ x ≤ 0.03) ceramics was measured from RT to T_d or 90 °C that is our equipment upper limit.

Table 2 shows the pyroelectric coefficient (p) and the figures of merit (*FOMs*) values of the NBT–0.06B_{1+x}T, (0.00 ≤ x ≤ 0.03) at RT, T_d or 90 °C. The p values varied with the Ba²⁺ content, and increased from 2.9 × 10⁻⁴ (C m⁻² °C⁻¹) to 3.54 × 10⁻⁴ (C m⁻² °C⁻¹) when x increased from 0.00 to 0.02 at RT. All the samples showed a great increase in p when the measurement temperature increased from 20 °C to T_d or 90 °C. This great increase in p at T_d or 90 °C was caused by the increase of I_p induced by the reorientation of ferroelectric domain and phase transition in MPB. When the temperature rises from RT to T_d , the phase transition from ferroelectric (*FR*) to relaxor antiferroelectric (relaxor *AFR*) started, and thus a sharp change in polarization resulted in a significant increase in p at T_d [15].

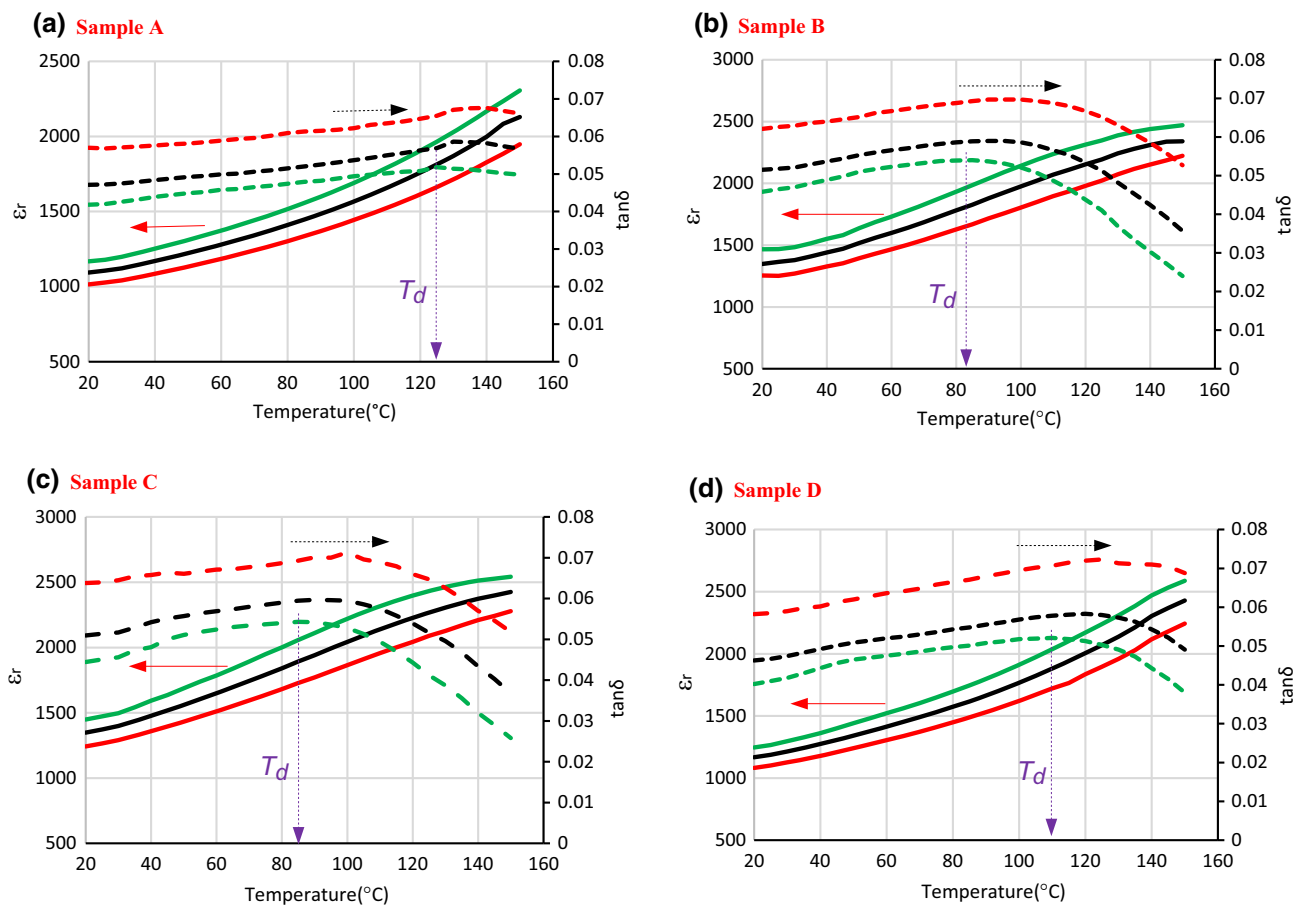


Fig. 3 The change of the relative permittivity (ϵ_r) and loss tangent ($\tan\delta$) with changing temperature ($^{\circ}\text{C}$) from RT up to 150°C , for the $\text{NBT}-0.06\text{B}_{1+x}\text{T}$, where $0.0 \leq x \leq 0.03$ from **a-d** in three different

The T_d for Sample B ($x = 0.01$) and C ($x = 0.02$) is below 90°C and for Sample A ($x = 0.00$) and D ($x = 0.03$) above 90°C , which explained why Sample B and C had a greater increase in p than Sample A and D. According to Anton et al. [7], the T_d determination depends on the highest value of the dielectric loss tangent, which may consistently generate higher T_d than other methods such as the thermally stimulated depolarization current; therefore the T_d for Sample A and D might actually be less than ~ 125 and $\sim 110^{\circ}\text{C}$, as a result that the observed increase in p for Sample A and D could be related to the beginning of the phase transition in these samples.

The increase of Ba content up to $x = 0.02$ reduces the distortion in the perovskite structure due to the replacement of Na^+ (1.39 \AA) by Ba^{2+} (1.61 \AA), which can shift the T_d to lower temperature [28]. Further increase in Ba content to $x = 0.03$ would lead to the appearance of a secondary phase or the replacement of Na^+ . Thus, the depolarization temperature at $x = 0.03$ shows a slight increase than that at $x = 0.01-0.02$ [14, 28, 30]. Table 2 also lists the p value ($4.14 \times 10^{-4} \text{ C m}^{-2} \text{ }^{\circ}\text{C}^{-1}$) of a typical PZT ceramic

frequencies (1, 10 and 100) kHz. The identified of the depolarization temperature (T_d) from the dielectric loss lines at 1 kHz

measured at RT as a reference. The prepared $\text{NBT}-0.06\text{B}_{1+x}\text{T}$ at $x = 0.01-0.03$ in this research show the comparable pyroelectric coefficients ($3.30-3.5 \times 10^{-4} \text{ C m}^{-2} \text{ }^{\circ}\text{C}^{-1}$) [5, 6, 9].

The values of F_i , F_v and F_D of the $\text{NBT}-0.06\text{B}_{1+x}\text{T}$ samples ($0.00 \leq x \leq 0.03$) at RT, T_d or 90°C are also shown in Table 2. The F_i value increased from $1.04 \times 10^{-10} \text{ (m/V)}$ ($x = 0.00$) to $1.24 \times 10^{-10} \text{ (m/V)}$ ($x = 0.02$) at RT and from $1.24 \times 10^{-10} \text{ (m/V)}$ ($x = 0.02$) to $260 \times 10^{-10} \text{ (m/V)}$ ($x = 0.02$) at T_d (85°C). The F_i of Sample C ($x = 0.02$) at RT is very close to that for PZT [$1.415 \times 10^{-10} \text{ (m/V)}$] [3]. However, at T_d (85°C) this sample ($x = 0.02$) shows a much higher p value [$260 \times 10^{-10} \text{ (m/V)}$] than the best value ($\sim 7.33 \times 10^{-10} \text{ (m/V)}$) at T_d (50°C) reported by Gue et al. [15].

The F_v values at RT and T_d or 90°C increased from $0.99 \times 10^{-2} \text{ (m}^2 \text{ }^{\circ}\text{C}^{-1}\text{)}$ at $x = 0.00$ to $1.05 \times 10^{-2} \text{ (m}^2 \text{ }^{\circ}\text{C}^{-1}\text{)}$ at $x = 0.03$. All these F_v values exceed the value for PZT [5, 15, 29, 30]. F_v values increased at T_d from 0.95×10^{-2} to $164 \times 10^{-2} \text{ m}^2/\text{C}$ for Sample C ($x = 0.02$).

Table 2 Comparing the pyroelectric coefficients and the figures of merit (F_i , F_v , and F_D) of the NBT–0.06B_{1+x}T(0.00 ≤ x ≤ 0.03) ceramic at frequency 1 kHz, at two different temperatures RT, T_d or 90 °C (due to equipment upper limit) with the other lead-free compositions and PZT

| Composition | p ($\times 10^{-4}$ C m ⁻² °C ⁻¹) at RT or T_d | F_i ($\times 10^{-10}$ m V ⁻¹) | F_v ($\times 10^{-2}$ m ² C ⁻¹) at f. 1 kHz | F_D ($\times 10^{-6}$ Pa ^{-1/2}) at f. 1 kHz | References |
|-----------------------------------|---|---|--|--|------------|
| NBT–0.06BT | 2.90 at RT | 1.04 at RT | 0.99 at RT | 8.6 at RT | This study |
| NBT–0.06BT | 55.3 at 90 °C | 19.7 at 90 °C | 14 at 90 °C | 75.6 at 90 °C | This study |
| NBT–0.06Ba_{1.01}T | 3.47 at RT | 1.238 at RT | 0.95 at RT | 7.7 at RT | This study |
| NBT–0.06Ba_{1.01}T | 601 at 85 °C | 215 at 85 °C | 115 at 90 °C | 674 at 90 °C | This study |
| NBT–0.06Ba_{1.02}T | 3.54 at RT | 1.244 at RT | 0.95 at RT | 8.3 at RT | This study |
| NBT–0.06Ba_{1.02}T | 741 at 85 °C | 260 at 85 °C | 164 at 85 °C | 915 at 85 °C | This study |
| NBT–0.06Ba_{1.03}T | 3.30 at RT | 1.177 at RT | 1.05 at RT | 9.1 at RT | This study |
| NBT–0.06Ba_{1.03}T | 73.1 at 90 °C | 26.12 at 90 °C | 15 at 90 °C | 83.9 at 90 °C | This study |
| PZT | 4.14 at RT | 1.415 at RT | 0.8 at RT | 9.01 | [5, 18] |
| NBT–0.07BZT | 5.7 at RT | 2.03 at RT | 2.18 at RT | 10.5 | [5, 18] |
| NBT–0.07BZT | 20.0 at 50 °C | 7.33 at 50 °C | 6.60 at 50 °C | 33.6 at 50 °C | [5, 18] |
| NBT–0.07BZT | 221 at 87 °C | – | – | – | [5, 18] |
| BNKBT | 3.25 at RT | 1.95 at RT | 2.6 at RT | 13.43 | [5, 18] |
| KNLNTS | 1.9 at RT | 0.931 at RT | 0.7 at RT | 11.5 | [5, 18] |

The samples made in this study are given in bold

The values of F_D at RT, T_d or 90 °C are shown in Table 2. The F_D values increased with extra Ba²⁺ content at RT from 8.6×10^{-6} Pa^{-1/2} (x = 0.00) to 9.2×10^{-6} Pa^{-1/2} (x = 0.03). Giant values for F_D achieved at T_d for Samples B and C were 674 and 915($\times 10^{-6}$ Pa^{-1/2}) respectively. F_D for PZT [5, 15, 29, 30] at RT is 9.01×10^{-6} Pa^{-1/2} and Sample D showed a higher F_D value than PZT (Table 2).

3 Conclusion

The NBT–0.06B_{1+x}T ceramics with extra Ba content were prepared by using conventional solid state synthesis route. The microstructure, dielectric, depolarization temperature and pyroelectric properties of these ceramics were dependent upon the Ba²⁺ content. The depolarization temperature shifted to around 85 °C with increasing the Ba²⁺ content up to x = 0.02. The pyroelectric coefficient and figures of merits (F_i , F_v , and F_D) all increase at RT when Ba²⁺ content increases to x = 0.02. The giant pyroelectric coefficient, 741×10^{-4} (C m⁻² °C⁻¹), was obtained at T_d when Ba²⁺ content increases to x = 0.02. The results for NBT–0.06B_{1+x}T obtained in this study indicate that NBT–0.06B_{1+x}T are promising candidates for pyroelectric applications in a wide temperature range.

Open Access This article is distributed under the terms of the Creative Commons Attribution 4.0 International License (<http://creativecommons.org/licenses/by/4.0/>), which permits unrestricted use, distribution, and reproduction in any medium, provided you give

appropriate credit to the original author(s) and the source, provide a link to the Creative Commons license, and indicate if changes were made.

References

1. Sustainable development and Environment EC Directive on WEEE and ROHS in electrical and electronic equipment. www.dti.gov.uk
2. T. Takenaka, K. Maruyama, K. Sakata, (Bi_{1/2}Na_{1/2}) TiO₃–BaTiO₃ system for lead-free piezoelectric ceramics. *Jap. J. Appl. Phys.* **30**, 2236 (1991). doi:10.1143/JJAP.30.2236
3. X. Wang, X. Tang, H. Chan, Electromechanical and ferroelectric properties of (Bi_{1/2} Na_{1/2}) TiO₃–(Bi_{1/2} K_{1/2}) TiO₃–BaTiO₃ lead-free piezoelectric ceramics. *Appl. Phys. Lett.* **85**, 91 (2004). doi:10.1063/1.1767592
4. X. Ma, L. Xue, L. Wan, S. Yin, Q. Zhou, Y. Yan, Synthesis, sintering, and characterization of BNT perovskite powders prepared by the solution combustion method. *Ceram. Int.* **39**, 8147–8152 (2013). doi:10.1016/j.ceramint.2013.03.088
5. S.T. Lau, C.H. Cheng, S.H. Choy, D.M. Lin, K.W. Kwok, H.L.W. Chan, Lead-free ceramics for pyroelectric applications. *J. Appl. Phys.* **103**, 10–13 (2008). doi:10.1063/1.2927252
6. S. Patel, A. Chauhan, S. Kundu, N.A. Madhar, B. Ilahi, R. Vaish, K.B.R. Varma, Tuning of dielectric, pyroelectric and ferroelectric properties of 0.715Bi_{0.5}Na_{0.5}TiO₃–0.065BaTiO₃–0.22SrTiO₃ ceramic by internal clamping. *AIP Adv.* **5**, 087145 (2015). doi:10.1063/1.4929328
7. E.M. Anton, W. Jo, D. Damjanovic, J. Rdel, Determination of depolarization temperature of (Bi_{1/2}Na_{1/2})TiO₃-based lead-free piezoceramics. *J. Appl. Phys.* **110**, 1–14 (2011). doi:10.1063/1.3660253
8. Y. Guo, M. Gu, H. Luo, Antiferroelectric phase and pyroelectric response in (Na_xBi_{2-x})Ti_{1-x}O_{3(1-x)}–xBaTiO₃ ceramics. *J. Am. Ceram. Soc.* **94**, 1350–1353 (2011). doi:10.1111/j.1551-2916.2011.04509.x

9. X.J. Li, Z.Z. Xi, W. Long, P.Y. Fang, Synthesis of antiferroelectric $(\text{Bi}_{0.534}\text{Na}_{0.5})_{0.94}\text{Ba}_{0.06}\text{TiO}_3$ ceramics with high phase transition temperature and broad temperature range by a solid-state reaction method. *Chin. Sci. Bull.* **58**, 2893–2897 (2013). doi:[10.1007/s11434-013-5972-2](https://doi.org/10.1007/s11434-013-5972-2)
10. J.-H. Cho, Y.-H. Jeong, J.-H. Nam, J.-S. Yun, Y.-J. Park, Phase transition and piezoelectric properties of lead-free $(\text{Bi}_{1/2}\text{Na}_{1/2})\text{TiO}_3$ - BaTiO_3 ceramics. *Ceram. Int.* **40**, 8419–8425 (2014). doi:[10.1016/j.ceramint.2014.01.051](https://doi.org/10.1016/j.ceramint.2014.01.051)
11. J. Suchanicz, U. Lewczuk, Effect of Ba addition on the structural, dielectric and ferroelectric properties of $\text{Na}_{0.5}\text{Bi}_{0.5}\text{TiO}_3$ ceramics. *Mater. Sci Poland* **33**, 414–417 (2015). doi:[10.1515/msp-2015-0056](https://doi.org/10.1515/msp-2015-0056)
12. M. Chen, Q. Xu, B.H. Kim, B.K. Ahn, J.H. Ko, W.J. Kang, O.J. Nam, Structure and electrical properties of $(\text{Na}_{0.5}\text{Bi}_{0.5})_{1-x}\text{Ba}_x\text{TiO}_3$ piezoelectric ceramics. *J. Eur. Ceram. Soc.* **28**, 843–849 (2008). doi:[10.1016/j.jeurceramsoc.2007.08.007](https://doi.org/10.1016/j.jeurceramsoc.2007.08.007)
13. C. Ma, X. Tan, Phase diagram of unpoled lead-free—ceramics. *Solid State Commun.* **150**, 1497–1500 (2010). doi:[10.1016/j.ssc.2010.06.006](https://doi.org/10.1016/j.ssc.2010.06.006)
14. Q. Li, J. Wang, L. Ma, H. Fan, Z. Li, Large electrocaloric effect in $(\text{Bi}_{0.5}\text{Na}_{0.5})_{0.94}\text{Ba}_{0.06}\text{TiO}_3$ lead-free ferroelectric ceramics by La_2O_3 addition. *Mater. Res. Bull.* **74**, 57–61 (2016). doi:[10.1016/j.materresbull.2015.10.010](https://doi.org/10.1016/j.materresbull.2015.10.010)
15. F. Guo, B. Yang, S. Zhang, F. Wu, D. Liu, P. Hu, Y. Sun, D. Wang, W. Cao, Enhanced pyroelectric property in $(1-x)(\text{Bi}_{0.5}\text{Na}_{0.5})\text{TiO}_3$ - $x\text{Ba}(\text{Zr}_{0.055}\text{Ti}_{0.945})\text{O}_3$: role of morphotropic phase boundary and ferroelectric-antiferroelectric phase transition. *Appl. Phys. Lett.* **103**, 182906 (2013). doi:[10.1063/1.4828675](https://doi.org/10.1063/1.4828675)
16. R.L. Byer, C.B. Roundy, Pyroelectric coefficient direct measurement technique and application to a nsec response time detector. *IEEE Trans. Sonics Ultrason.* **19**, 333–338 (1972). doi:[10.1109/T-SU.1972.29679](https://doi.org/10.1109/T-SU.1972.29679)
17. C. Xu, D. Lin, K.W. Kwok, Structure, electrical properties and depolarization temperature of $(\text{Bi}_{0.5}\text{Na}_{0.5})\text{TiO}_3$ - BaTiO_3 lead-free piezoelectric ceramics. *Solid State Sci.* **10**, 934–940 (2008). doi:[10.1016/j.solidstatesciences.2007.11.003](https://doi.org/10.1016/j.solidstatesciences.2007.11.003)
18. M. Rawat, K.L. Yadav, A. Kumar, P.K. Patel, N. Adhlakha, J. Rani, Structural, dielectric and conductivity properties of Ba^{2+} doped $(\text{Bi}_{0.5}\text{Na}_{0.5})\text{TiO}_3$ ceramic, advanced. *Mater. Lett.* **3**, 286–292 (2012). doi:[10.5185/amlett.2012.2322](https://doi.org/10.5185/amlett.2012.2322)
19. M.S. Yoon, N.H. Khansur, S.C. Ur, The effect of pre-milling/pre-synthesis process and excess Ba on the microstructure and dielectric/piezoelectric properties of nano-sized $0.94[(\text{Bi}_{0.5}\text{Na}_{0.5})\text{TiO}_3]$ - $0.06[\text{Ba}_{(1+x)}\text{TiO}_3]$. *Ceram. Int.* **36**, 1265–1275 (2010). doi:[10.1016/j.ceramint.2010.01.011](https://doi.org/10.1016/j.ceramint.2010.01.011)
20. Y. Hiruma, K. Yoshii, H. Nagata, T. Takenaka, Investigation of phase transition temperatures on $(\text{Bi}_{1/2}\text{Na}_{1/2})\text{TiO}_3$ - $(\text{Bi}_{1/2}\text{K}_{1/2})\text{TiO}_3$ and $(\text{Bi}_{1/2}\text{Na}_{1/2})\text{TiO}_3$ - BaTiO_3 lead-free piezoelectric ceramics by electrical measurements. *Ferroelectrics* **346**, 114–119 (2007). doi:[10.1080/00150190601180471](https://doi.org/10.1080/00150190601180471)
21. R. Ranjan, A. Dviwedi, Structure and dielectric properties of $(\text{Na}_{0.5}\text{Bi}_{0.5})_{1-x}\text{Ba}_x\text{TiO}_3$: $0 \leq x \leq 0.10$. *Solid State Commun.* **135**, 394–399 (2005). doi:[10.1016/j.ssc.2005.03.053](https://doi.org/10.1016/j.ssc.2005.03.053)
22. E. Sapper, S. Schaab, W. Jo, T. Granzow, J. Rödel, Influence of electric fields on the depolarization temperature of Mn-doped $(1-x)\text{Bi}_{1/2}\text{Na}_{1/2}\text{TiO}_3$ - $x\text{BaTiO}_3$. *J. Appl. Phys.* **111**, 014105 (2012). doi:[10.1063/1.3674275](https://doi.org/10.1063/1.3674275)
23. S. Zhang, A.B. Kounga, E. Aulbach, W. Jo, T. Granzow, H. Ehrenberg, J. Rödel, Lead-free piezoceramics with giant strain in the system $\text{Bi}_{0.5}\text{Na}_{0.5}\text{TiO}_3$ - BaTiO_3 - $\text{K}_{0.5}\text{Na}_{0.5}\text{NbO}_3$. II. Temperature dependent properties. *J. Appl. Phys.* **103**, 034108 (2008). doi:[10.1063/1.2838476](https://doi.org/10.1063/1.2838476)
24. W. Jo, J.E. Daniels, J.L. Jones, X. Tan, P.A. Thomas, D. Damjanovic, J. Rödel, Evolving morphotropic phase boundary in lead-free $(\text{Bi}_{1/2}\text{Na}_{1/2})\text{TiO}_3$ - BaTiO_3 piezoceramics. *J. Appl. Phys.* **109**, 014110 (2011). doi:[10.1063/1.3530737](https://doi.org/10.1063/1.3530737)
25. W. Jo, J. Daniels, D. Damjanovic, W. Kleemann, J. Rdel, Two-stage processes of electrically induced-ferroelectric to relaxor transition in $0.94(\text{Bi}_{1/2}\text{Na}_{1/2})\text{TiO}_3$ - 0.06BaTiO_3 . *Appl. Phys. Lett.* **102**, 4 (2013). doi:[10.1063/1.4805360](https://doi.org/10.1063/1.4805360)
26. X. Li, P. Liu, Z. Xi, P. Fang, W. Long, X. Zhao, Effects of doping Bi and Nd on the phase transition and electric properties of $(\text{Bi}_{1/2}\text{Na}_{1/2})_{0.94}\text{Ba}_{0.06}\text{TiO}_3$ ceramics. *J. Electroceram.* **32**, 86–91 (2014). doi:[10.1007/s10832-013-9881-1](https://doi.org/10.1007/s10832-013-9881-1)
27. Q. Xu, D.P. Huang, M. Chen, W. Chen, H.X. Liu, B.H. Kim, Effect of bismuth excess on ferroelectric and piezoelectric properties of a $(\text{Na}_{0.5}\text{Bi}_{0.5})\text{TiO}_3$ - BaTiO_3 composition near the morphotropic phase boundary. *J. Alloys Compd.* **471**, 310–316 (2009). doi:[10.1016/j.jallcom.2008.03.078](https://doi.org/10.1016/j.jallcom.2008.03.078)
28. S.R. Shannigrahi, F.E.H. Tay, K. Yao, R.N.P. Choudhary, Effect of rare earth (La, Nd, Sm, Eu, Gd, Dy, Er and Yb) ion substitutions on the microstructural and electrical properties of sol-gel grown PZT ceramics. *J. Eur. Ceram. Soc.* **24**, 163–170 (2004). doi:[10.1016/S0955-2219\(03\)00316-9](https://doi.org/10.1016/S0955-2219(03)00316-9)
29. Y.Z. Zhu, S.P. Lin, Y. Zheng, D.C. Ma, B. Wang, Improvement of pyroelectric figures of merit in zirconia-doped congruent lithium niobate single crystals. *J. Mater. Sci.* **51**, 3155–3161 (2016). doi:[10.1007/s10853-015-9625-5](https://doi.org/10.1007/s10853-015-9625-5)
30. J. Abe, M. Kobume, T. Nishimura, T. Yazaw, Y. Nakai, Effects of manganese addition on pyroelectric properties of $(\text{Bi}_{0.5}\text{Na}_{0.5}\text{TiO}_3)_{0.94}(\text{BaTiO}_3)_{0.06}$ ceramics. *Integr. Ferroelectr.* **80**, 87–95 (2006). doi:[10.1080/10584580600656502](https://doi.org/10.1080/10584580600656502)